International Journal of Applied
and Natural Sciences (IJANS)
ISSN(P): 2319-4014; ISSN(E): 2319-4022
Vol. 8, Issue 4, Jun - Jul 2019; 71-80

International Academy of Science,
Engineering and Technology
Connecting Researchers; Nurturing Innovations

ELECTRON TEMPERATURE AND ELECTRON DENSITY OF ATMOSPHERIC PRESSURE NEEDLE TO PLANE DIELECTRIC BARRIER DISCHARGE AIR PLASMA

M K Alam[1], M W Rahman[2] & A T M Kaosar Jamil[3]

[1]Research Scholar, Department of Physics, Pabna University of Science & Technology, Pabna, Bangladesh

[2]Research Scholar, Department of Applied Physics & Electronic Engineering, University of Rajshahi, Rajshahi, Bangladesh

[3]Research Scholar, Department of Physics, Dhaka University of Engineering & Technology, Gazipur, Bangladesh

ABSTRACT

Electron temperature and electron density of atmospheric pressure single dielectric barrier discharges in the 'needle-air gap-glass barrier-plane' configuration are investigated by means of optical emission spectroscopy (OES). The atmospheric pressure open-air diffuse type sustainable plasma is generated by a high voltage (5 kV) AC source operating at a frequency of 20 kHz. The electron temperature is estimated using the spectral line intensity ratio method and the electron density is determined using Stark broadening parameters. It was found that the electron temperature and electron density both decrease with the increase of gap distance and dielectric thickness. It is also found that the electron temperature is less than 1 eV (0.61–0.33 eV) and electron density is 1.80×10^{13} – 7.21×10^{11} cm^{-3} depending upon air gap and dielectric thickness.

KEYWORDS: *Atmospheric Pressure Plasma; Dielectric Barrier; Needle to Plane; Diffuse Discharge; Optical Emission Spectroscopy, Spectral Line*

Article History

Received: *05 May 2019* | ***Revised:*** *21Jun 2019* | ***Accepted:*** *28 Jun 2019*

INTRODUCTION

For producing atmospheric pressure non-thermal plasma, dielectric barrier discharge (DBD) is the most effective method [1]. The main feature of DBD is to establish the non-equilibrium discharge at atmospheric pressure in an economic and sustainable way [2]. Generation and uses of open air plasma are investigated with growing interest because of its cost-effectiveness and more convenient alternative to low-pressure plasma technology [3]. Many configurations of DBD and the applications of air plasma have been studied in this regards. Capacitive coupled radio-frequency (RF) discharges are investigated for material processing and surface treatment [3] or plasma display panels [4]. Now a day, scientists are searching for uniform and appropriate 'Bio-compatible' room temperature sustainable plasma source in atmospheric pressure for material processing and at the same time for the treatment of biological materials. The DBD geometry with a single dielectric barrier does not allow the charges to accumulate the electrode surface and all the charges to move into the electrical system [5]. The typical materials like glass, quartz, ceramics, alumina, and polymers with low dielectric loss and relatively high breakdown strength can serve this purpose [5].

Needle to plane single dielectric barrier plasma source has been discovered and characterized by means of various plasma diagnostic methods [6–8]. The needle to plane dielectric barrier discharge showed higher power consumption and higher discharge current than the conventional DBD type at a given voltage. For this reason, the needle to plane geometry of DBD is more efficient than the conventional DBD [9]. The produced plasma remains at room temperature with stable diffuse discharge. Electrode configuration plays an important role in this case. Needle to plane DBD has been used to increase the material processing rate by increasing the plasma density [10].

The electron temperature and electron density with gas temperature are the most fundamental parameters in atmospheric pressure plasma discharges to understand the physics of plasmas. To determine the electron temperature and electron density, different methods can be used. Langmuir probe diagnostics method is common for atmospheric pressure [11] but it is difficult because of the small plasma dimension, electrode configuration, the non-thermal behavior and strong collision processes of the plasma. The plasma parameters can be determined properly by using optical emission spectroscopic (OES) techniques. De-Zheng Yang *et al* [12] studied the effects of pulse peak voltage, pulse repetition rate and the gap distance between electrodes on gas temperature and the emission intensities of NO, OH and N_2 in the needle-plate atmospheric pressure nanosecond barrier discharge plasma using OES. Using the single needle-plate electrode configuration at atmospheric pressure a diffuse bi-directional pulsed dielectric barrier discharge (BNPDBD) is investigated in the air [13].

The physical mechanism of the needle to plane DBD discharge is yet to understand clearly and many factors like the influence of source voltage, electrode geometry, discharge gap, and dielectric thickness need further investigation. Mangolini et al [14] investigated the influence of dielectric thickness on density profiles of Helium under an AC power supply. The research on the influence of dielectric thickness and discharge gap on-air plasma discharge by OES are relatively few in number. Therefore the study of the effect of the air gap and dielectric thickness on the performance of the needle to plane atmospheric pressure DBD plasma parameters by OES is essential.

The optical diagnosis for electron temperature and electron density of AC pulsed needle to plane single dielectric barrier open air plasma at atmospheric pressure with different air gap and dielectric thicknesses are presented in this article. The aim of the present research work is to get control over plasma parameters for the optimum condition of plasma discharges to be used for material processing and for biomedical applications. Using OES methods the line ratio technique is used to measure the electron temperature (T_e) of the produced plasma and electron density (n_e) is measured using stark broadening of spectra by Voigt fitting. The line-ratio techniques are used for calculations of atmospheric pressure low-temperature plasmas [15]. Detail experimental setup, analytical results, and discussions are given in the following sections.

Experimental Setup

Figure 1 shows the schematic diagram of the experimental arrangement (needle-airgap-glass-plane) of the atmospheric pressure dielectric barrier discharge (APDBD) in the open air.

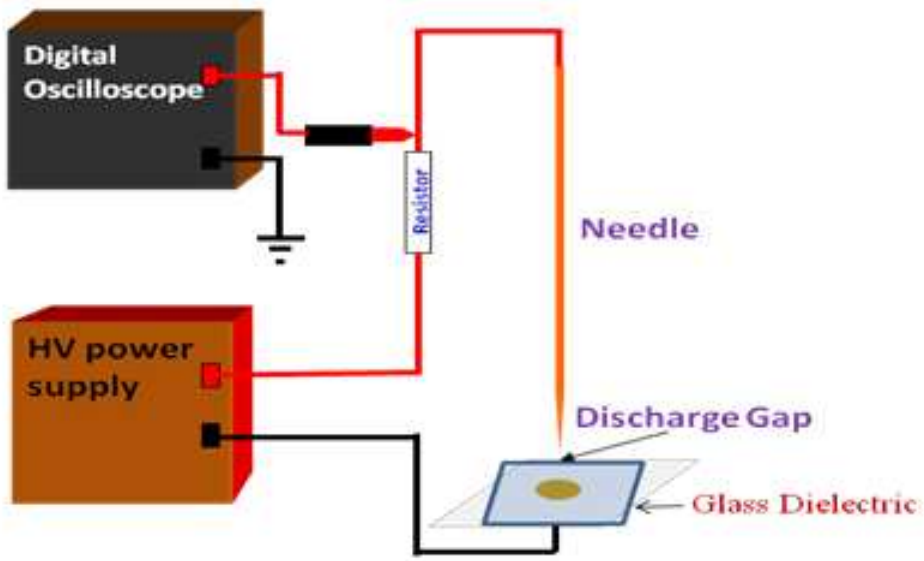

Figure 1: Schematic Diagram of Atmospheric Pressure Needle-to-Plane Dielectric Barrier Discharge

The discharge is made between a floating needle electrode of diameter 0.2 mm and a silver plate electrode of diameter 3 mm with a gap distance 0.5–1.0 mm. The electrodes were connected toahighvoltage5 kV power supply operating ata frequency of 20 kHz. The plate electrode is covered with a single dielectric barrier (glass) of 0.15–0.75 mm thickness. The produced air plasma is diffuse type and stable in nature as shown in Figure 2. A Tektronix (Beaverton, OR) TDS-5000 series 350 MHz 4-channel digital oscilloscope monitors the power delivered to the circuit. An HVP-08 high voltage probe (1:1000) is used to monitor the peak to peak voltage. The current flowing through the plasma is measured by a current probe ($CP-07C$).

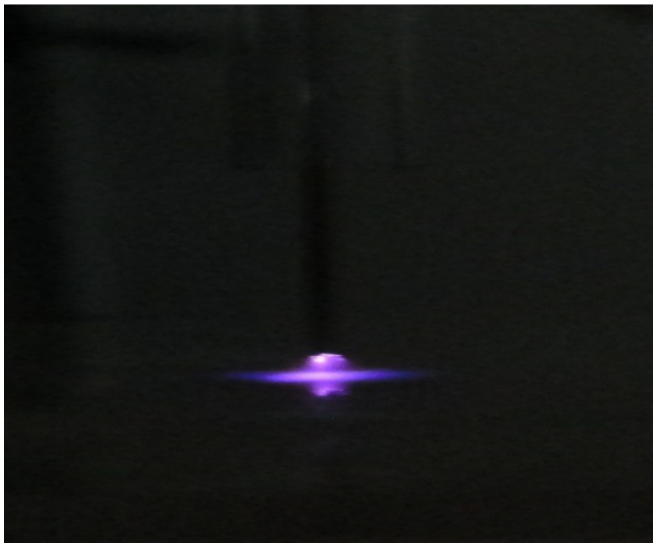

Figure 2: Camera View of Needle-to-Plane APDBD Plasma

Emitted spectrum from the produced plasma is fed to the spectrometer (USB2000+XR1) through a 200 cm long optical fiber cable. The spectrometer is associated with a computer for spectral data acquisition. The discharge voltages, currents, and emitted spectra are recorded for different air gap and different dielectric thicknesses in order to investigate the properties of the produced air plasma. The recorded emission spectra along with the identified major peaks of the species

are depicted in Figure 3. The analytical results are discussed in the following sections.

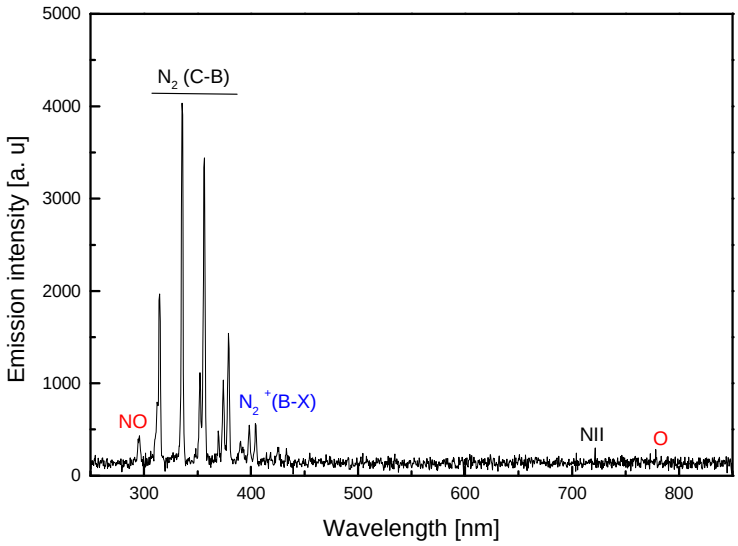

Figure 3: Emission Spectra of Air Plasma with 1.0 Mm Air Gap, 0.45 mm Dielectric Thickness 5 kv Source Voltage And 20 khz Frequency

Optical Diagnosis

Electron Temperature

Electron temperature can directly reflect the average kinetic energy of the electrons in the plasma. To understand the physics of plasma it is an important parameter. Xiaozhi Shen *et al* [16] used intensity ratios between lines of the *2p3p – 2p3s* and *2p4f–2p3d* transition arrays for temperature diagnostics. For pin-to-plane atmospheric pressure air plasma Liu *et al* [17] measured the electron temperature T_e by using the electrical method with Einstein's equation $\frac{kT_e}{e} = \frac{D_e}{\mu_e}$ where k is the Boltzmann constant ($1.38 \times 10^{23} JK^{-1}$), D_e is the electron diffusion constant and μ_e is the electron drift mobility. The ratio of D_e and μ_e can be expressed as a function of E/N [18–19].

In this experiment, the line intensity ratio method is used to evaluate T_e assuming that the population densities of the upper levels of the considered lines follow the Boltzmann distributions. The ratio of the intensities of two lines at λ_{pq} and λ_{rs} is simply given as [20]

$$\frac{I_1}{I_2} = \left(\frac{\lambda_{rs}}{\lambda_{pq}}\right)\left(\frac{g_p}{g_r}\frac{A_{pq}}{A_{rs}}\right)\exp\left[-\frac{E_p - E_r}{K_B T_e}\right] \quad (1)$$

Where g and A represent the statistical weight (of the lower state of the line) and Einstein coefficient respectively. In this experiment, NIII emission lines of wavelength 335.878 and 374.595 nm are used to calculate the electron temperature T_e by equation (1). The values of g_p, g_r, A_{pq}, A_{rs}, E_p and E_r are taken from the National Institute of Standards and Technology (NIST) database. From the above database, it is seen for 335.878 nm, the transition takes place from 2s2p3p to 2s2p3s level whose term symbols are ^4P and $^4P^0$, respectively. The 374.595 nm transition takes place between the same levels with term symbols from ^4S to $^4P^0$. The J value of the upper level of the 1st transition is 1/2 and that of the 2nd transition is 3/2. It is found that the electron temperature varies from 0.618 to 0.3365 eV depending upon the air gap

and dielectric thickness. This dependency is shown in Figure 4, which show that T_e decrease with increasing air gap and dielectric (glass) thickness.

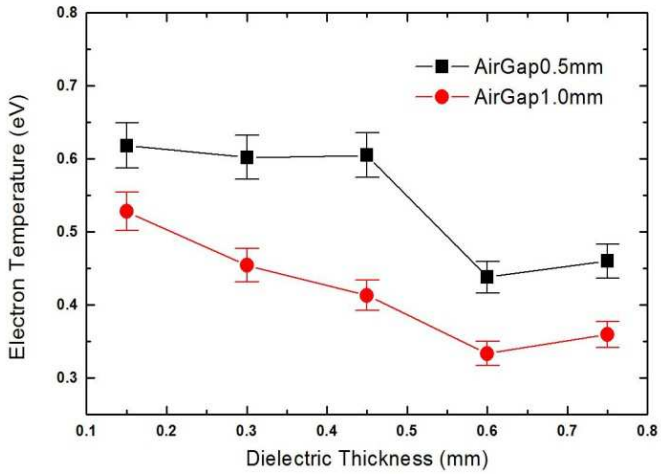

Figure 4: Variation of Electron Temperature with Dielectric Thickness

When the air gap increases, the value of pd (where p is the pressure and d is the air gap) increases because the pressure is constant at atmospheric pressure and the electric field across the air gap decreases. The atoms and molecules experience less kinetic energy and more difficult to breakdown. For this reason electron density and mean kinetic energy of ions and electrons decrease with the increase of air gap. Therefore, the collision frequency between electrons and molecules decreases and few numbers of excited molecules, ions, and electrons are generated. As a result, the average kinetic energy of electrons decreases with an increasing air gap. Hence the electron temperature T_e decreases with an increasing air gap. The electron temperature decrease with increasing dielectric thickness and can be explained by the equation $Q = C_d V$ where, $C_d = \frac{\epsilon_0 \epsilon_r A}{d}$ where d is the dielectric thickness.

Electron Density

The electron density is a fundamental plasma parameter and plays a significant role in understanding the discharge physics and optimization of the operation of plasmas [21,22]. Different methods (Langmuir probe [23], microwave interferometry [24], Laser Thomson scattering (LTS) [25] and Optical Emission Spectroscopy [26] are used to measure the electron density in plasma. For atmospheric pressure low-temperature discharge, both the probe and the microwave-based methods are difficult to use due to small plasma dimensions and strong collision processes. LTS is effective but very difficult because of its complicated experimental setup [27]. On the other hand, the OES-based technique has the advantages of being non-intrusive, inexpensive and convenient. There are three major OES techniques to determine the electron density in low-temperature plasmas. In one OES method involves the use of the Stark broadening of emission line profiles [28], another is to analyze the continuum radiation if it is observed [29] and the last one is the line ratio method, in which the intensity ratio of emission lines is related to the electron density [30]. Here in this experiment, the electron density is measured by the Stark broadening technique.

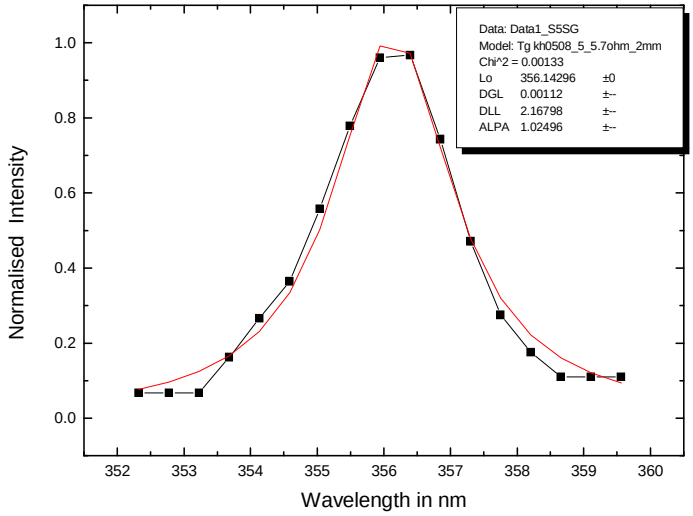

Figure 5: Recorded Spectral Line and Voigt Fit

Interactions of electrons with ions are responsible [31] for Stark broadening, but electrons play a significant role due to their lower masses and higher relative velocities. During OES data analyses, it is obtained that the contributions of Natural broadening and Resonance broadening are found negligible, but the dependence of van der Waals broadening is on average 30% on Lorentz profile. Stark broadening is caused by the Coulomb interaction of the charged particles present in the plasma. Electron number density is evaluated by using Stark broadening technique with selected spectral line (356.397 nm) of Oxygen. It is known that the full width at half maximum (FWHM) of a Stark broadened line is related to electron density [32] as,

$$\Delta\lambda_{Stark}=2.5\times10^{-10}\alpha n_e^{2/3}(nm) \quad (2)$$

Where n_e is in cm^{-3} and α is the ion broadened parameter. The values of α are obtained from the least square curve fitting of the Voigt profiles (Figure 5).

In this experiment, the electron density is estimated using equation (2). It is found that the electron density decreases with increasing air gap and dielectric thickness within the range from 1.80×10^{13} cm^{-3} to 7.21×10^{11} cm^{-3} as shown in Figure 6. With an increasing air gap, the electrons gain less energy from the decreased electric fields and the ionizing collisions between electrons and neutrals become less frequent and hence the production of free electron decrease. At the same time, the low-energy electrons play a dominant role in the electron-impact population transfer process between excited species. On the other hand when dielectric thickness increases, the electric resistance increases between the electrodes and the electric field decrease inside the air gap and therefore electron density decrease.

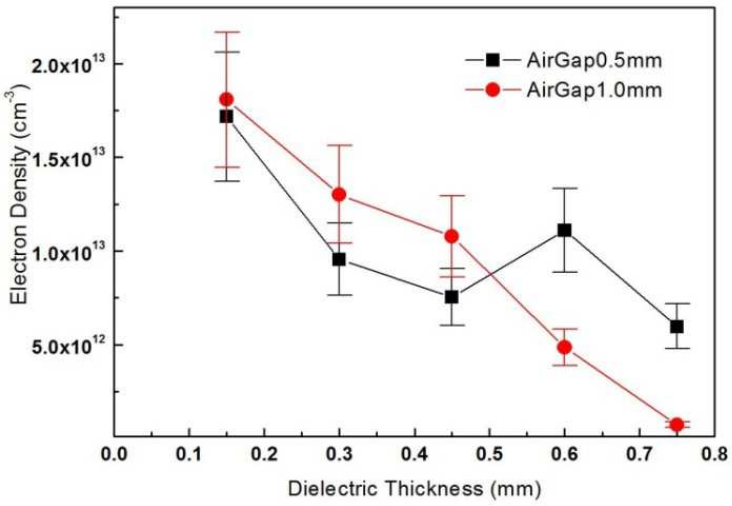

Figure 6: Variation of Electron Density with Dielectric Thickness

Figure 6 also shows an increase of electron density near 0.6mm dielectric thickness when the electrode gap is 0.5mm and then it is again shows decreasing with increasing dielectric thickness. This may be due to the secondary electron emission from the dielectric surface around dielectric thickness 0.6mm at lower electrode gap.

CONCLUSIONS

Atmospheric pressure single dielectric barrier in the 'needle-plane glass barrier' configuration pulsed air plasma with 0.5–1.0 mm air gap and 0.15–0.75 mm dielectric thickness have been produced. The produced plasma was diffused shape and stable. Optical emission spectroscopy is used to diagnose the produced plasma. The air gap and dielectric thickness between the electrodes appreciably influence the discharge plasma. The emission intensity increases with increasing air gap within the range of gap 0.5–1.0 mm at fixed dielectric thickness. The electron temperature and electron density decrease with increasing dielectric thickness and air gap. The measured electron temperature from 0.618 to 0.3346 eV and electron density from 1.80×10^{13} to 7.21×10^{11} cm^{-3}, respectively with 0.5 to 1.0 mm air gap and 0.15 to 0.75 mm dielectric thickness. The produced diffuse type stable air plasma is non-thermal and suitable for biomedical applications and material processing.

ACKNOWLEDGEMENTS

The research work is done in the Plasma Science & Technology Lab., Department of Applied Physics and Electronic Engineering, the University of Rajshahi under the full guidance of Prof. Dr. M R Talukder. Researcher N C Roy also helped in the experimental process with his homemade plasma source.

REFERENCES

1. *A Gulec, and L Oksuz, Characteristics of Dielectric Barrier Discharge, in AIP Conference Proceedings, **04**, 899(1), 697 (2007).*
2. *2. M. Y. Naz, A. Ghafiar, N. U. Rehman, S. Shukrullah, and M. A. Ali, Progress In Electromagnetics Research M, Vol**. 24**, 193-207 (2012).*
3. *3. J Park, I Henins, H W Herrmann, G S Selwyn, and R F Hicks, J. Appl. Phys. **89**, 20 (2001).*
4. *Schutze, A., Jeong, J. Y., Babayan, S. E., Park, J., Selwyn, G. S., & Hicks, R. F. (1998). The atmospheric-pressure plasma jet: a review and comparison to other plasma sources. IEEE transactions on plasma science, 26(6), 1685-1694*
5. *H Yoshiki, and Y Horiike, Japan J. Appl. Phys. **40**, L360 (2001).*
6. *W I Wiese, Plasma Diagnostic Techniques, edited by R H Haddlestone and S I Leonar; **pp-369-377** (Academic, New York, 1965).*
7. *E Stoffels, A J Flikweert, W W Stoffels, and G M W Kroesen, Plasma Sources Sci. Technol. **11**, 383 (2002).*
8. *I E Kieft, E P Van der Laan, and E Stoffels, New J. Phys. **6**, 149 (2004).*
9. *8. E Stoffels, R E J Sladek, I E Kieft, H Kesten, and H Wiese, Plasma Phys. Control. Fusion, **46**, B167 (2004).*
10. *Se-Jin Kyung et al, Surface & Coatings Technology **202**, 1204–1207 (2007).*
11. *Y H Lee, S J Kyung, C H Jeong, and G Y Yeom; Jpn. J. Appl. Phys., Part 2 **44,** L78 (2004).*
12. *M R Talukder, D. Korzec, and M. Kando, J. Appl. Phys. **91**: 9529-9538 (2002).*
13. *De-Zheng Yang, Yang Yang, Shou-Zhe Li, Dong-Xia Nie, Shuai Zhang, and Wen-ChunWang, Plasma Sources Sci. Technol. **21**, 035004 (9pp) (2012).*
14. *De-zheng Yang, Wen-chun Wang, Li Jia, Dong-xia Nie, and Heng-chao Shi, JOURNAL OF APPLIED PHYSICS **109**, 073308 (2011).*
15. *L Mangolini, C. Anderson, and J. Heberlein, J. Phys. D **37**, 1021 (2004).*
16. *Xi-Ming Zhu and Yi-Kang Pu, J. Phys. D: Appl. Phys. **43** (2010) 403001 (24pp).*
17. *Xiaozhi Shen et al, The Astrophysical Journal, **801**:129 (11pp), (2015 March 10).*
18. *Z J Liu et al, Spectrochimica Acta Part A: Molecular and Biomolecular Spectroscopy **121**, 698–703 (2014).*
19. *T Shao, K Long, C Zhang, P Yan, S Zhang, and R Pan, J. Phys. D: Appl. Phys. **41**, 215203 (2008).*
20. *K Takaki, M Hosokawa, T Sasaki, S Mukaigawa, and T Fujiwara, Appl. Phys. Lett. **151** (2005).*
21. *H J Kunze, Introduction to Plasma Spectroscopy, Springer (July 2009).*
22. *M A Lieberman, and A J Lichtenberg, Principles of Plasma Discharges and Materials Processing 2nd edn (New York: Wiley) (2005).*

23. *F F Chen, Introduction to Plasma Physics and Controlled Fusion 2nd edn (New York: Plenum)(1984).*
24. *K V A Godya, IEEE Trans. Plasma Sci.* ***34****, 755 (2006).*
25. *G A Hebner, E V Barnat, P A Miller, A Paterson, and J P Mand Holland, Plasma Sources*
26. *Sci. Technol.****15****, 879 (2006).*
27. *H Kempkens, and J Uhlenbusch, Plasma Sources Sci. Technol.* ***9****, 492 (2000).*
28. *V M Donnelly, J. Phys. D: Appl. Phys.* ***37****, R217 (2004).*
29. *S G Belostotskiy, R Khandelwal, Q Wang, V M Donnelly, D J Economou, and N Sadeghi, Appl. Phys. Lett.* ***92*** *221507 (2008).*
30. *J Torres, J M Palomares, A Sola, JJAMand, v d Mullen, and A Gamero, J. Phys. D: Appl. Phys.* ***40****, 5929 (2007).*
31. *R F G Meulenbroeks, M F M Steenbakkers, Z Qing, M C Mand van de Sanden, and D C Schram, Phys. Rev. E* ***49*** *2272 (1994).*
32. *X M Zhu, and Y K Pu, J. Phys. D: Appl. Phys.* ***40****, 2533 (2007).*
33. *M Moravej, X. Yang, R. F. Hicks, J. Penelon, and S. E. Babayan, J. Appl. Phys.* ***99****, 093305-6 (2006).*
34. *R H Huddlestone, and S L Leonard, Plasma Diagnostic Techniques, Academic Press, New York (1965).*